

Theoretical analysis of magnetic Raman scattering in La_2CuO_4 : Two-magnon intensity with the inclusion of ring exchange

A. A. Katanin^{1,2} and A. P. Kampf¹

¹*Institut für Physik, Theoretische Physik III, Elektronische Korrelationen und Magnetismus, Universität Augsburg, 86135 Augsburg, Germany*

²*Institute of Metal Physics, 620219 Ekaterinburg, Russia*

(Received 3 December 2002; published 25 March 2003)

We evaluate the Raman light-scattering intensity for the square lattice Heisenberg antiferromagnet with plaquette ring exchange J_{\square} . With the exchange couplings as fixed before from an accurate fit to the spin-wave dispersion in La_2CuO_4 , leading in particular to $J_{\square} = 0.24J$, we demonstrate in a parameter-free calculation that the inclusion of the plaquette exchange contribution to the dispersion and the magnon-magnon interaction vertex gives a peak position in B_{1g} scattering geometry $E_{\max} = 2.71J$ which is in excellent agreement with the experimental data. Yet, the intrinsic width and the line shape of the two-magnon remain beyond a description in terms of a spin-only Hamiltonian.

DOI: 10.1103/PhysRevB.67.100404

PACS number(s): 75.40.Gb, 75.10.Jm, 76.60.Es

The magnetic properties of La_2CuO_4 have been a subject of many detailed investigations over the last decade. Understanding this undoped parent compound of high-temperature superconducting cuprates is a precondition for the many theories which describe metallic cuprates by doping carriers into a layered antiferromagnet. The conventional starting point for undoped cuprates is the two-dimensional (2D) spin-1/2 Heisenberg model with nearest-neighbor (nn) exchange interaction J .¹ Despite substantial progress on the theory of the 2D Heisenberg antiferromagnet,² some of the experimental facts for La_2CuO_4 have clearly demonstrated that a complete description of the magnetic excitations requires additional physics not contained in the 2D Heisenberg model with J only. Examples include the asymmetric line shape of the two-magnon Raman intensity³ or the infrared optical absorption.⁴

The importance of an additional ring (plaquette)-exchange coupling for La_2CuO_4 recently found direct experimental support from the observed dispersion of the spin waves along the magnetic Brillouin-zone boundary.⁵ A fit of the experimental results⁵ using the theoretical spin-wave dispersion, which consistently includes quantum renormalization effects,⁶ has provided accurate values for the nn exchange integral $J = 1720$ K and the ring-exchange coupling $J_{\square} = 0.24J$. The new estimate for J corrects previous values which have been used in past years and which were consistently 10–15 % lower. Also the value for J_{\square} must be considered surprisingly large, but the spin stiffness and the Néel temperature calculated with the new parameter set obtained in Ref. 6 were in excellent agreement with the experimental data and thereby confirmed the deduced exchange-coupling parameters. The value of the ring exchange J_{\square} also agreed with the strong-coupling expansion studies of the three-band Hubbard model in the parameter range relevant for CuO_2 planes.⁷

The Heisenberg model with J only was previously found insufficient to describe the experimentally observed asymmetry and width of the Raman spectra of undoped cuprate compounds.³ The Raman spectrum of the Heisenberg model

was investigated within the ladder approximation for the magnon-magnon scattering vertex many years ago^{8,9} and gave an almost symmetric narrow peak located at $E_{\max} = 3.3J$. It was shown⁹ that magnon self-energy and vertex corrections to the ladder approximation as well as four-magnon scattering contributions are small and negligible. Numerically, the problem was investigated by series expansions around the Ising limit,¹⁰ exact diagonalizations on small clusters,¹¹ and QMC calculations.¹² The results of these studies led to a peak position and a two-magnon line shape, which were very close to the spin-wave results. Furthermore, the value of the exchange integral $J = 1440$ K for La_2CuO_4 , as extracted from the position of the two-magnon Raman peak, appears too small in comparison to early neutron-scattering results for the spin-wave spectrum ($J = 1650$ K), see Ref. 13, and references therein.

The asymmetric line shape of the two-magnon Raman intensity³ has led to proposals that spin-phonon interactions,^{14–16} resonant phenomena,^{17,18} purely fermionic contributions,¹⁹ or cyclic ring exchange^{20–22} need to be included beyond the nn Heisenberg model. A possible importance of ring exchange for Raman scattering was conjectured also from numerical calculations²³ which showed that a finite J_{\square} gives rise to additional high-energy contributions in the Raman intensity—yet with little spectral weight.

The accurate estimates for the exchange couplings therefore demand a theoretical reanalysis of two-magnon scattering in La_2CuO_4 , which we investigate in the present paper with an emphasis on the effects of ring exchange. The question that we address is that to what extent the values for the exchange parameters—including the finite J_{\square} —consistently describe the two-magnon intensity in La_2CuO_4 and whether the Heisenberg model with ring exchange alone is sufficient to explain the experimentally observed line shape of the Raman intensity. To answer this question, we calculate the magnon-magnon interaction vertex in the presence of the ring-exchange term and then solve the ladder equation for the Raman-scattering vertex.

We start with the Heisenberg model on a square lattice with ring-exchange coupling,^{23–25}

$$\begin{aligned}
H = & J \sum_{i,\delta} \mathbf{S}_i \cdot \mathbf{S}_{i+\delta} + J' \sum_{i,\delta'} \mathbf{S}_i \cdot \mathbf{S}_{i+\delta'} + J'' \sum_{i,\delta''} \mathbf{S}_i \cdot \mathbf{S}_{i+\delta''} + J_{\square} \\
& \times \sum_{\langle ijkl \rangle} [(\mathbf{S}_i \cdot \mathbf{S}_j)(\mathbf{S}_k \cdot \mathbf{S}_l) + (\mathbf{S}_i \cdot \mathbf{S}_l)(\mathbf{S}_k \cdot \mathbf{S}_j) \\
& - (\mathbf{S}_i \cdot \mathbf{S}_k)(\mathbf{S}_j \cdot \mathbf{S}_l)], \quad (1)
\end{aligned}$$

where J, J' , and J'' are the first (δ), second (δ'), and third (δ'') nearest-neighbor in-plane exchanges. We use the Dyson-Maleev representation for the spin operators

$$\begin{aligned}
S_i^+ &= \sqrt{2S} a_i, \quad S_i^z = S - a_i^\dagger a_i, \quad i \in A, \\
S_i^- &= \sqrt{2S} \left(a_i^\dagger - \frac{1}{2S} a_i^\dagger a_i^\dagger a_i \right), \quad i \in A, \quad (2)
\end{aligned}$$

$$\begin{aligned}
S_j^+ &= \sqrt{2S} b_j^\dagger, \quad S_j^z = -S + b_j^\dagger b_j, \quad j \in B, \\
S_j^- &= \sqrt{2S} \left(b_j - \frac{1}{2S} b_j^\dagger b_j b_j \right), \quad j \in B, \quad (3)
\end{aligned}$$

where A and B denote the two sublattices of the antiferromagnet; a_i^\dagger, a_i , and b_j^\dagger, b_j are Bose operators and $S = 1/2$. With the Bogoliubov transformation

$$\begin{aligned}
a_{\mathbf{k}} &= u_{\mathbf{k}} \alpha_{\mathbf{k}} + v_{\mathbf{k}} \beta_{\mathbf{k}}^\dagger, \\
b_{\mathbf{k}} &= u_{\mathbf{k}} \beta_{\mathbf{k}} + v_{\mathbf{k}} \alpha_{\mathbf{k}}^\dagger;
\end{aligned}$$

and by introducing the ‘‘coherence factors’’

$$\begin{aligned}
u_{\mathbf{k}} &= [(A_{\mathbf{k}} + E_{\mathbf{k}})/(2E_{\mathbf{k}})]^{1/2}, \\
v_{\mathbf{k}} &= -[(A_{\mathbf{k}} - E_{\mathbf{k}})/(2E_{\mathbf{k}})]^{1/2},
\end{aligned}$$

we diagonalize the quadratic part of the Hamiltonian and obtain the spin-wave spectrum (for details, see Ref. 6)

$$E_{\mathbf{k}} = \sqrt{A_{\mathbf{k}}^2 - B_{\mathbf{k}}^2}, \quad (4)$$

$$\begin{aligned}
A_{\mathbf{k}} &= 4S[J\gamma - J'\gamma'(1 - \nu_{\mathbf{k}}^{\delta'}) - J_{\square} S^2(\gamma_0^{\square} + \gamma_{\delta'}^{\square} \nu_{\mathbf{k}}^{\delta'})] \\
& - 4J'' S \gamma'' (1 - \nu_{\mathbf{k}}^{\delta''}), \quad (5)
\end{aligned}$$

$$B_{\mathbf{k}} = 4S(J\gamma - J_{\square} S^2 \gamma_{\delta}^{\square}) \nu_{\mathbf{k}}^{\delta}, \quad (6)$$

with the momentum-dependent coefficients

$$\begin{aligned}
\nu_{\mathbf{k}}^{\delta} &= (\cos k_x + \cos k_y)/2, \quad \nu_{\mathbf{k}}^{\delta'} = \cos k_x \cos k_y, \\
\nu_{\mathbf{k}}^{\delta''} &= (\cos 2k_x + \cos 2k_y)/2. \quad (7)
\end{aligned}$$

Note that the quantum renormalization factors $\{\gamma_{\delta}\}$ in Eq. (4) take into account the renormalization of the magnon spectrum due to quartic terms.⁶ The resulting Hamiltonian reads

$$\begin{aligned}
H = & \sum_{\mathbf{k}} E_{\mathbf{k}} (\alpha_{\mathbf{k}}^\dagger \alpha_{\mathbf{k}} + \beta_{\mathbf{k}}^\dagger \beta_{\mathbf{k}}) \\
& + \sum V_{\mathbf{k}_1 \mathbf{k}_2; \mathbf{k}_3 \mathbf{k}_4}^{klmn} : R_{\mathbf{k}_1, k}^\dagger R_{\mathbf{k}_2, l}^\dagger R_{\mathbf{k}_3, m} R_{\mathbf{k}_4, n} : \delta_{\mathbf{k}_1 + \mathbf{k}_2, \mathbf{k}_3 + \mathbf{k}_4}, \quad (8)
\end{aligned}$$

where we used the vector notation

$$R_{\mathbf{k}} = (\alpha_{\mathbf{k}}, \beta_{-\mathbf{k}}^\dagger) \quad (9)$$

and $k, l, m, n = 1, 2$. The quartic part in Eq. (8) is normal ordered, since all ‘‘Hartree-Fock’’ renormalizations are already absorbed in the quadratic part of the Hamiltonian, cf. Ref. 26.

We use the effective Loudon-Fleury²⁷ Hamiltonian in B_{1g} geometry for the coupling of the incoming and outgoing photons to the localized nn spins which are involved in the two-spin-flip Raman process

$$H_R = \Lambda \sum_j \mathbf{S}_j \cdot (\mathbf{S}_{j+\delta_y} - \mathbf{S}_{j+\delta_x}); \quad (10)$$

$\delta_{x(y)}$ are unit vectors in the directions x, y , respectively, and Λ is a coupling constant that includes the electric-field vectors of the two photons. For the calculation of the Raman light-scattering intensity in the ladder approximation for repeated magnon-magnon scattering processes only, the vertex $V_{\mathbf{k}\mathbf{k}'; \mathbf{k}'\mathbf{k}}^{(4)} = V_{\mathbf{k}\mathbf{k}'; \mathbf{k}'\mathbf{k}}^{1,2,1,2}$ is needed.^{8,9} The complicated vertex function $V_{\mathbf{k}_1 \mathbf{k}_2; \mathbf{k}_3 \mathbf{k}_4}^{1,2,1,2}$ was calculated with the help of computer algebra. After Bogoliubov transformation, the ring-exchange term in Eq. (1) gives 1057 (!) contributions with different combinations of α and β operators. The general result for the vertex $V_{\mathbf{k}_1 \mathbf{k}_2; \mathbf{k}_3 \mathbf{k}_4}^{(4)}$ is rather involved, however, for equal momenta it simplifies to

$$V_{\mathbf{k}\mathbf{k}'; \mathbf{k}'\mathbf{k}}^{(4)} = \frac{B_{\mathbf{k}-\mathbf{k}'}(A_{\mathbf{k}} A_{\mathbf{k}'} + E_{\mathbf{k}} E_{\mathbf{k}'}) - A_{\mathbf{k}-\mathbf{k}'} B_{\mathbf{k}} B_{\mathbf{k}'} - R_{\square}}{2E_{\mathbf{k}} E_{\mathbf{k}'}} \quad (11)$$

where the effects of the ring-exchange coupling are included in the magnon spectrum (4) and in the additional vertex contribution,

$$\begin{aligned}
R_{\square} = & 8J_{\square} [B_{\mathbf{k}} B_{\mathbf{k}'} (4 + \nu_{\mathbf{k}}^{\delta'} + \nu_{\mathbf{k}'}^{\delta'} + \nu_{\mathbf{k}-\mathbf{k}'}^{\delta'}) \\
& - 2A_{\mathbf{k}'} B_{\mathbf{k}} (\nu_{\mathbf{k}'}^{\delta} + \nu_{\mathbf{k}, \mathbf{k}-\mathbf{k}'}^{\square}) - 2A_{\mathbf{k}} B_{\mathbf{k}'} (\nu_{\mathbf{k}}^{\delta} + \nu_{\mathbf{k}-\mathbf{k}', \mathbf{k}'}^{\square}) \\
& + 2A_{\mathbf{k}} A_{\mathbf{k}'} (\nu_{\mathbf{k}-\mathbf{k}'}^{\delta} + \nu_{\mathbf{k}, \mathbf{k}'}^{\square}) + 2E_{\mathbf{k}} E_{\mathbf{k}'} (-\nu_{\mathbf{k}-\mathbf{k}'}^{\delta} + \nu_{\mathbf{k}, \mathbf{k}'}^{\square})] \quad (12)
\end{aligned}$$

and $\nu_{\mathbf{k}, \mathbf{k}'}^{\square} = (\cos k_x \cos k'_y + \cos k_y \cos k'_x)/2$.

The first two terms in the numerator of Eq. (11) coincide with the corresponding result for the 2D nn Heisenberg antiferromagnet^{8,9} but with renormalized coefficients $A_{\mathbf{k}}$, $B_{\mathbf{k}}$, and the renormalized magnon dispersion $E_{\mathbf{k}}$ in Eq. (4). The time-ordered response function of two-magnon Raman scattering is given by

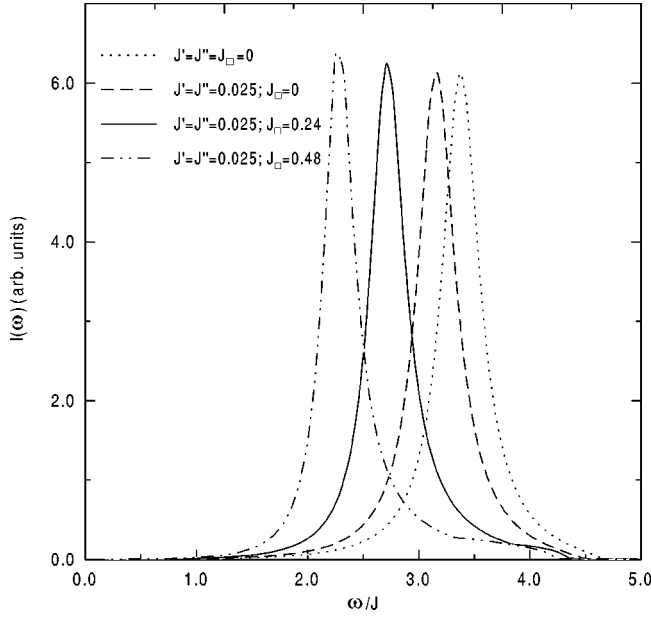


FIG. 1. Evolution of the two-magnon Raman intensity with increasing ring-exchange couplings; different parameter sets are indicated in the figure.

$$G(\omega) = \int_{-\infty}^{\infty} dt e^{i\omega t} \langle T[H_R(t)H_R(0)] \rangle,$$

where $H_R(t)$ is the Heisenberg representation of H_R , Eq. (10). The Raman light-scattering intensity is then determined by $I(\omega) = -(1/\pi) \text{Im} G(\omega)$. In the ladder approximation, we obtain the following equations:^{8,9}

$$G(\omega) = i\Lambda^2 \int \frac{d\omega'}{2\pi} \sum_{\mathbf{k}} \frac{A_{\mathbf{k}} f_{\mathbf{k}}}{E_{\mathbf{k}}} G_{\alpha}^{(0)}(\mathbf{k}, \omega + \omega') \Gamma_{\mathbf{k}}(\omega), \quad (13)$$

$$\Gamma_{\mathbf{k}}(\omega) = \frac{f_{\mathbf{k}} A_{\mathbf{k}}}{E_{\mathbf{k}}} - i \int \frac{d\omega_1}{2\pi} \sum_{\mathbf{k}_1} V_{\mathbf{k}\mathbf{k}_1; \mathbf{k}_1\mathbf{k}}^{(4)} G_{\alpha}^{(0)}(\mathbf{k}_1, \omega + \omega_1) \Gamma_{\mathbf{k}_1}(\omega), \quad (14)$$

where $G_{\alpha, \beta}^{(0)}(\mathbf{k}, \omega) = -1/(E_{\mathbf{k}\mp} \omega - i0^+)$ and $f_{\mathbf{k}} = \cos k_x - \cos k_y$. The result reads

$$G(\omega) = \frac{\Lambda^2 L_2(\omega)}{D(\omega)} \left\{ 1 + \frac{J}{2} \left[L_0(\omega) - \frac{L_1^2(\omega)}{L_2(\omega)} \right] \right\}, \quad (15)$$

$$D(\omega) = 1 + (J - 2J_{\square} S^2) \frac{L_2(\omega)}{2} + (J + 6J_{\square} S^2) \frac{L_0(\omega)}{2} + (J - 2J_{\square} S^2)(J + 6J_{\square} S^2) \frac{L_0(\omega)L_2(\omega) - L_1^2(\omega)}{4}, \quad (16)$$

where

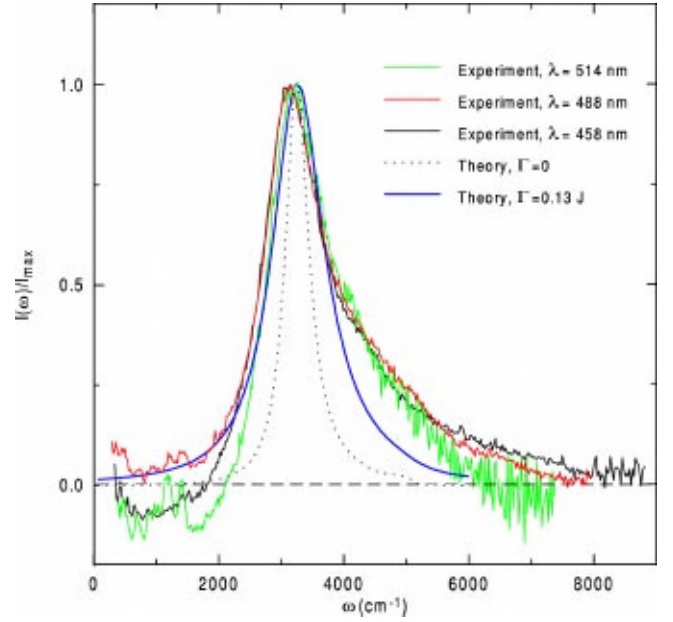


FIG. 2. Comparison of the theoretical result without ($\Gamma = 0$) and with additional damping ($\Gamma = 0.13J$) to the experimental Raman intensity in La_2CuO_4 in B_{1g} geometry taken from Ref. 3. Calculations were performed with the parameter set (16). The three experimental curves belong to different incoming photon frequencies; the high-energy intensity background was subtracted. All datasets were normalized to their corresponding intensity maximum.

$$L_m(\omega) = i \int \frac{d\omega'}{2\pi} \sum_{\mathbf{k}} \frac{f_{\mathbf{k}}^2 A_{\mathbf{k}}^m}{E_{\mathbf{k}}^m} G_{\alpha}^{(0)}(\mathbf{k}, \omega + \omega') G_{\beta}^{(0)}(\mathbf{k}, \omega') = \sum_{\mathbf{k}} \frac{f_{\mathbf{k}}^2 A_{\mathbf{k}}^m}{E_{\mathbf{k}}^m} \frac{1}{\omega - 2E_{\mathbf{k}}}. \quad (17)$$

For $J_{\square} = 0$, the above formulas reduce to the known results of Refs. 8 and 9.

For the numerical calculations, we use the parameter set determined in Ref. 6 from the fit to the spin-wave dispersion

$$J = 151.9 \text{ meV}, \quad J' = J'' = 0.025J, \quad J_{\square} = 0.24J. \quad (18)$$

For these exchange couplings, the renormalization parameters follow as⁶

$$\gamma = 1.158, \quad \gamma' = 0.909, \quad \gamma'' = 0.852;$$

$$\gamma_{\square}^{\square} = 2.220, \quad \gamma_{\delta}^{\square} = 1.971, \quad \gamma_{\delta'}^{\square} = 1.721. \quad (19)$$

Nevertheless, we first explore the J_{\square} dependence of the two-magnon Raman intensity as shown in Fig. 1. On varying J_{\square} , the renormalization parameters (19) necessarily have to be recalculated each time. For $J' = J'' = J_{\square} = 0$, the result in Fig. 1 coincides with that obtained in Refs. 8 and 9. In a first step we turn on J' and J'' and observe a shift of the two-magnon peak position to lower frequencies and a further downward shift when also the ring-exchange coupling is added. The magnitude of the peak shift due to the ring exchange is quite strong. In addition, due to the finite J_{\square} , the spectrum near the upper edge of the two-magnon continuum develops a

“foot” structure. For comparison, we also plot the Raman-scattering intensity for a twice larger ring exchange $J_{\square} = 0.48J$, where the above effects are even more pronounced. The position of the peak estimated with $J_{\square} = 0.24J$ is $E_{\max} = 2.71J$ and with the absolute values in Eq. (18) is therefore an excellent agreement with the experimental result,³ $E_{\max} = 2.65J = 3150 \text{ cm}^{-1}$. If we turn off the vertex contribution R_{\square} in Eq. (11) and therefore keep only the influence of the ring exchange in the spin-wave dispersion, we obtain $E_{\max} = 2.86J$ which is still much smaller than the peak position without ring exchange ($E_{\max} = 3.15J$). Therefore, the modification of the spectrum due to a finite J_{\square} is the major origin for the peak shift to lower energies.

In Fig. 2, we compare the Raman line shape, obtained for the parameter set (18) with the experimental data on La_2CuO_4 from Ref. 3. Although the precise peak position is in excellent agreement with the data, its width is only slightly influenced by ring-exchange coupling. The foot structure near the upper edge of the spectrum does result from ring exchange and therefore indeed leads to an asymmetry of the line shape, its weight, however, is too small to account for the overall linewidth and line shape. As in the case $J_{\square} = 0$ we expect four-magnon contributions to be quantitatively small.⁹ Therefore, other processes must contribute which are not described by the Heisenberg model with ring exchange alone. It was proposed that the damping due to spin-phonon coupling^{14–16} is responsible for the peak width which in the current calculation is underestimated by roughly a factor of 2. In order to incorporate extrinsic sources for damping beyond the extended Heisenberg Hamiltonian, Eq.

(1), we have introduced a small damping Γ into the denominators of $L_m(\omega)$, Eq. (17). As a reasonable choice, Γ is assumed constant over the entire Brillouin zone because it is predominantly the zone-boundary magnons that determine the shape of the two-magnon peak. We plot the result of this calculation for $\Gamma = 0.13J$ in Fig. 2. One can see that while the width of the experimentally observed spectra can be fitted in such a way, the asymmetry of the spectrum is not accounted for. Since the Raman spectra do depend on the incoming light frequency,²⁹ the two-magnon scattering is identified as a resonant process and therefore an additional source for the strong asymmetry of the line shape is expected to arise from the coupling to the charge degrees of freedom.^{17,18,28}

In summary, we have investigated the effect of ring exchange on two-magnon Raman scattering in the 2D Heisenberg antiferromagnet. Using the previously fixed exchange coupling parameter set we find in a fit-parameter free calculation an excellent agreement with the position of the two-magnon peak in La_2CuO_4 . This reconfirms the magnitude of the ring-exchange coupling $J_{\square} = 0.24J$ in this material. Ring-exchange creates additional high energy spectral weight in the Raman intensity, but J_{\square} alone is insufficient to explain the overall asymmetric line shape and linewidth. The recently proposed modification of the Raman operator¹⁶ might affect the line shape and remains to be explored for $J_{\square} > 0$.

It is a pleasure to thank T. Kopp, T. Nunner, and G. Uhrig for insightful discussions. We acknowledge support through Sonderforschungsbereich 484 of the Deutsche Forschungsgemeinschaft.

-
- ¹E. Manousakis, *Rev. Mod. Phys.* **63**, 1 (1991).
²S. Chakravarty, B.I. Halperin, and D.R. Nelson, *Phys. Rev. B* **39**, 2344 (1989).
³K.B. Lyons *et al.*, *Phys. Rev. B* **39**, 9693 (1989); S. Sugai *et al.*, *ibid.* **42**, 1045 (1990).
⁴J.D. Perkins *et al.*, *Phys. Rev. Lett.* **71**, 1621 (1993).
⁵R. Coldea, S.M. Hayden, G. Aeppli, T.G. Perring, C.D. Frost, T.E. Mason, S.-W. Cheong, and Z. Fisk, *Phys. Rev. Lett.* **86**, 5377 (2001).
⁶A.A. Katanin and A.P. Kampf, *Phys. Rev. B* **66**, 100403(R) (2002).
⁷E. Müller-Hartmann and A. Reischl, *Eur. Phys. J. B* **28**, 173 (2002).
⁸R.W. Davies, S.R. Chinn, and H.J. Zeiger, *Phys. Rev. B* **4**, 992 (1971).
⁹C.M. Canali and S.M. Girvin, *Phys. Rev. B* **45**, 7127 (1992).
¹⁰R.R.P. Singh *et al.*, *Phys. Rev. Lett.* **62**, 2736 (1989).
¹¹E. Dagotto and D. Poilblanc, *Phys. Rev. B* **42**, 7940 (1990); E. Dagotto and S. Bacci, *ibid.* **42**, 8772 (1990).
¹²A.W. Sandvik *et al.*, *Phys. Rev. B* **57**, 8478 (1998).
¹³V.Yu. Irkhin, A.A. Katanin, and M.I. Katsnelson, *Phys. Rev. B* **60**, 1082 (1999).
¹⁴P. Knoll *et al.*, *Phys. Rev. B* **42**, 4842 (1990).
¹⁵F. Nori, R. Merlin, S. Haas, A.W. Sandvik, and E. Dagotto, *Phys. Rev. Lett.* **75**, 553 (1995).
¹⁶P.J. Freitas and R.R.P. Singh, *Phys. Rev. B* **62**, 5525 (2000).
¹⁷A. Chubukov and D. Frenkel, *Phys. Rev. Lett.* **74**, 3057 (1995).
¹⁸F. Schönfeld, A.P. Kampf, and E. Müller-Hartmann, *Z. Phys. B: Condens. Matter* **102**, 25 (1997).
¹⁹C.-M. Ho, V.N. Muthukumar, M. Ogata, and P.W. Anderson, *Phys. Rev. Lett.* **86**, 1626 (2001).
²⁰Y. Honda, Y. Kuramoto, and T. Watanabe, *Phys. Rev. B* **47**, 11 329 (1993).
²¹J. Eroles, C.D. Batista, S.B. Bacci, and E.R. Gagliano, *Phys. Rev. B* **59**, 1468 (1999).
²²J. Lorenzana, J. Eroles, and S. Sorella, *Phys. Rev. Lett.* **83**, 5122 (1999).
²³M. Roger and J.M. Delrieu, *Phys. Rev. B* **39**, 2299 (1989).
²⁴M. Takahashi, *J. Phys. C* **10**, 1289 (1977).
²⁵A.H. MacDonald, S.M. Girvin, and D. Yoshioka, *Phys. Rev. B* **41**, 2565 (1990); **37**, 9753 (1988).
²⁶E. Rastelli and A. Tassi, *Phys. Rev. B* **11**, 4711 (1975).
²⁷P.A. Fleury and R. Loudon, *Phys. Rev.* **166**, 514 (1969).
²⁸S. Basu and A. Singh, *Phys. Rev. B* **54**, 6356 (1996).
²⁹G. Blumberg *et al.*, *Phys. Rev. B* **53**, R11930 (1996).